JOC The Journal of Organic Chemistry

pubs.acs.org/joc Article

Ascandinines A–D, Indole Diterpenoids, from the Sponge-Derived Fungus *Aspergillus candidus* HDN15-152

Guoliang Zhou, Chunxiao Sun, Xuewen Hou, Qian Che, Guojian Zhang, Qianqun Gu, Chenguang Liu, Tianjiao Zhu,* and Dehai Li*

Cite This: *J. Org. Chem.* 2021, 86, 2431–2436 Read Online

ACCESS | Metrics & More | Article Recommendations | Supporting Information

ABSTRACT: Four new indole diterpenoids, ascandinines A–D (**1**–**4**), were isolated from an Antarctic sponge-derived fungus *Aspergillus candidus* HDN15-152. Their structures, including absolute configurations, were established based on NMR data, computational calculations, and biosynthetic considerations. Ascandinine A (**1**) possesses an unprecedented 2-oxabicyclo[2.2.2]octan-3-ol motif embedded in a pentacyclic ring system, while compounds **2**–**4** represent a rare type of indole diterpenoid featuring the 6/5/5/6/6/6/6-fused ring system. Compound **3** displayed anti-influenza virus A (H1N1) activity with an IC_{50} value of 26 μM, while compound **4** showed cytotoxicity against HL-60 cells with an IC_{50} value of 7.8 μM.

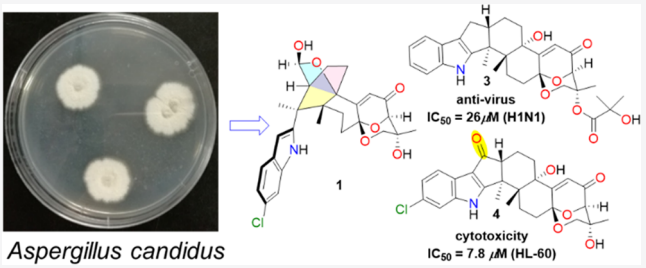

INTRODUCTION

The paxilline-like indole diterpenoids, featuring a 6/5/5/6/6/6 hexacyclic ring system, are biogenetically derived from tryptophan and geranylgeranyl diphosphate (GGPP) and are one of the largest classes of fungal indole terpenoids.[1] Although the base carbon skeleton is invariable, the diversity of paxilline-like indole diterpenoids is enhanced not only by different levels of further prenylation at various positions but also by oxidation, hydroxylation, and other extended modifications.[2−5] Consistent with this large structural diversity, the paxilline-like indole diterpenoids show broad biological activities, such as cytotoxicity, antiviral and PTP1B inhibitory effects.[6−13]

In our ongoing search for new biologically active metabolites from Antarctic-derived fungi,[14−16] the fungus *Aspergillus candidus* HDN15-152 was isolated from an unidentified sponge collected from Prydz Bay. Further examination led to the discovery of four new indole diterpenoids, named ascandinines A–D (**1**–**4**). Ascandinine A (**1**) possesses an unprecedented indole-substituted 6/6/6/6/6 pentacyclic skeleton with a 2-oxabicyclo[2.2.2]octan-3-ol motif, which is structurally derived from the cleavage of the C-17 and C-18 bond in the paxilline-like indole diterpenoids (Figure 1). Compounds **2**–**4** represent a rare type of indole diterpene skeleton characterized by the 6/5/5/6/6/6/6-fused ring system, with only four previous examples (asperindoles A–D) reported.[4] Compound **3** displayed anti-influenza virus A (H1N1) activity with an IC_{50} value of 26 μM (ribavirin as a positive control, IC_{50} = 31 μM), and compound **4** showed cytotoxicity against HL-60 cell lines with an IC_{50} value of 7.8 μM. Herein, we report the isolation, structure elucidation, and bioactivities of these compounds.

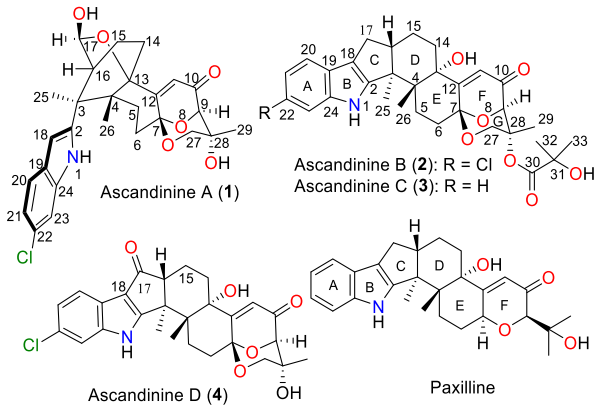

Figure 1. Structures of compounds **1**–**4** and paxilline.

RESULTS AND DISCUSSION

The fungal strain *A. candidus* HDN15-152 was fermented (30 L) under static conditions at 28 °C for 30 days. The EtOAc extract (35.5 g) of the fermentation was fractionated by repeated silica gel chromatography, C-18 column chromatography (CC), Sephadex LH-20 column chromatography, ODS

Received: October 29, 2020
Published: January 20, 2021

MPLC, and finally high-performance liquid chromatography (HPLC) to yield compounds **1**−**4**.

Ascandinine A (**1**) was isolated as a white solid. Its molecular formula was established as $C_{27}H_{30}ClNO_6$ on the basis of high-resolution electrospray ionization mass spectrometry (HRESIMS) data ($[M + H]^+$ ion at *m/z* 500.1835, calcd for 500.1834) and requiring 13° of unsaturation. The ^{13}C NMR data along with the DEPT spectrum revealed the presence of 27 carbons including one carbonyl carbon, five sp^2 and five sp^3 hybrid quaternary carbons, five sp^2 and three sp^3 hybrid methines, five sp^3 methylenes, and three methyls. The indole unit was elucidated based on the heteronuclear multiple bond correlation (HMBC) from H-21 (δ_H 6.93) to C-19 (δ_C 126.3)/C-23 (δ_C 110.8), H-20 (δ_H 7.43) to C-18 (δ_C 99.1)/C-22 (δ_C 125.3)/C-24 (δ_C 137.0), H-23 (δ_H 7.36) to C-19, H-18 (δ_H 6.24) to C-2 (δ_C 147.2)/C-19/C-24, and from NH-1 (δ_H 10.97) to C-2/C-18/C-19 (Figure 2). Further analysis of the

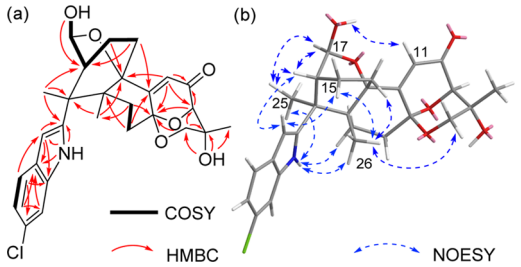

Figure 2. (a) COSY and key HMBC correlations and (b) key NOESY correlations for **1**.

NMR data of **1** to those of asperindole A indicated that they shared a similar substructure (rings E, F, and G).[4] The tricyclic ring system (rings E, F, and G) was further confirmed by the HMBC correlations from H-5 (δ_H 2.12, 1.96) to C-6 (δ_C 30.5)/C-13 (δ_C 77.6), from H-6 (δ_H 2.14, 1.92) to C-4 (δ_C 40.0)/C-7 (δ_C 93.4)/C-12 (δ_C 158.9), from H-11 (δ_H 6.45) to C-7/C-9 (δ_C 83.6)/C-10 (δ_C 196.3)/C-13, from H-27 (δ_H 3.59, 3.54) to C-7/C-9/C-28 (δ_C 64.6), and from OH-28 (δ_H 5.30) to C-27 (δ_C 68.7)/C-28/C-29 (δ_C 21.6). The cyclohexane ring D was extended by the HMBC correlations from H-25 (δ_H 1.38) to C-16 (δ_C 40.2), from H-26 (δ_H 0.88) to C-3 (δ_C 44.1)/C-4/C-13, from H-14 (δ_H 2.20, 2.14) to C-12/C-16, and from H-15 (δ_H 2.09) to C-13 as well as COSY correlations of H-14/H-15/H-16 (δ_H 2.28). The connectivity of C-2 and C-3 was deduced via HMBC correlations from H-25 to C-2/C-16. Reanalysis of the NMR data revealed one unassigned methine (δ_C 91.6, C-17) and one exchangeable proton at δ_H 6.64 (OH-17). The COSY correlations of H-16/H-17 (δ_H 5.30)/OH-17 and the HMBC correlation from OH-17 to C-16 indicated that the hydroxylated C-17 was connected to C-16. Considering the molecular formula, an extra ring was required to fulfill the 13° of unsaturation, and one ether linkage between C-13 and C-17 was also suggested according to the chemical shifts of H-17 (δ_H 5.30), C-17 (δ_C 91.6), and C-13 (δ_C 77.6) as well as the NOESY correlation of OH-17/H-11 (Figure 2).

The relative configuration of **1** was assigned on the basis of NOESY correlations (Figure 2) and ^{13}C NMR calculations (Figure 3). The key NOESY correlations of H-26/H-14/H-15 and H-25/H-16/H-17 indicated that Me-26 is in spatial proximity to C-14/C-15 while Me-25 faces C-17 in the 2-oxabicyclo[2.2.2]octane motif. The NOEs between H-26 and

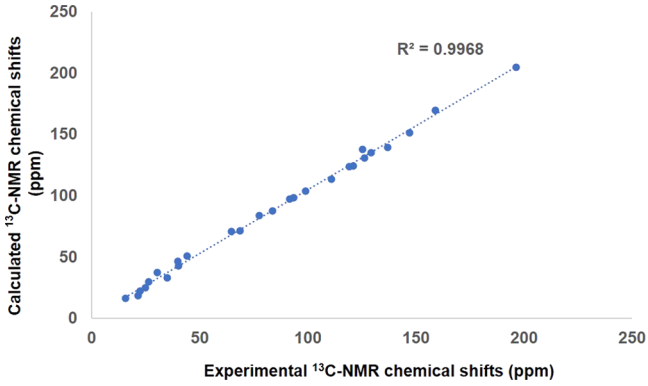

Figure 3. Linear correlations between the calculated and experimental ^{13}C NMR chemical shifts for compound **1**.

H-27 indicated that Me-26 and CH_2-27 are on the same side of ring E. Due to the chemical shifts of C-28 (δ_C 64.6), CH-9 (δ_C 83.6, δ_H 3.83), and Me-29 (δ_C 21.6, δ_H 0.80), as well as biosynthetic considerations, the relative configurations of C-28 and C-9 were suggested to be the same as those of **2**−**4** (Table 1) and asperindole A.[4] Due to the complexity of compound **1**, the planar structure and relative configuration of **1** were further confirmed by comparison of experimental (Table S4) and density functional theory (DFT)-calculated (Figure 3) ^{13}C NMR data.[17] The absolute configuration of compound **1** was further deduced by comparison of the calculated data (Figure 4), and experimental electronic circular dichroism (ECD) spectra revealed the absolute configuration of **1** was 3*S*, 4*R*, 7*R*, 9*R*, 13*S*, 16*R*, 17*S*, 28*R*.

The molecular formulae of ascandinines B (**2**), C (**3**), and D (**4**) were determined to be $C_{31}H_{36}ClNO_7$, $C_{31}H_{37}NO_7$, and $C_{27}H_{28}ClNO_6$, respectively, by HRESIMS. The ^1H and ^{13}C NMR data of ascandinine B (**2**) (Table 1) showed considerable resemblance to those of asperindole A.[4] The main difference between **2** and asperindole A was the presence of a cluster of signals for a 2-hydroxy-2-methylpropanoate unit deduced by the HMBC correlations from H-32 (δ_H 1.38)/H-33 (δ_H 1.38) to C-30 (δ_C 176.1) and C-31 (δ_C 72.0) and from OH-31 (δ_H 5.25) to C-30, C-31, and C-33 (δ_C 27.8) (Figure 5). The 2-hydroxy-2-methylpropanoate side chain was located at C-28 (δ_C 75.6) via oxygen, as suggested by the molecular weight and the chemical shifts of C-28. The coupling constants and multiplicity of the aromatic protons (δ_H 7.26, d, J = 8.0 Hz, H-20; δ_H 6.89, t, J = 7.1 Hz, H-21; δ_H 6.93, t, J = 7.2 Hz, H-22; and δ_H 7.26, d, J = 8.0 Hz, H-23) in ring A and the 2D NMR data (Figure S1) allowed the conclusion that ascandinine C (**3**) is a dechlorinated analogue of **2**. Analysis of the ^1H and ^{13}C NMR spectra of ascandinine D (**4**) suggested that its structure was closely related to that of ascandinine B (**2**) with the main differences being the replacement of CH_2-17 in **2** (δ_C 27.5) by a ketone carbonyl group in **4** (δ_C 195.4, C-17) and of the 2-hydroxy-2-methylpropanoate in **2** by a hydroxyl group in **4**, supported by the HMBC correlations from 28-OH (δ_H 5.32) to C-28 (δ_C 65.6)/C-29 (δ_C 21.2) (Figure S2).

The relative configuration of **2** was deduced as 3*S**, 4*R**, 7*R**, 9*R**, 13*S**, 16*S**, 28*R** according to the NOESY correlations of H-26 (δ_H 1.01)/H-16 (δ_H 2.71), H-25 (δ_H 1.31)/OH-13 (δ_H 5.15), H-26/H-27 (δ_H 4.09, 3.69), and H-29 (δ_H 1.22)/H-11 (δ_H 6.12) (Figure 5). The calculated ECD curve for **2** matched well with the experimental one (Figure 4),

https://dx.doi.org/10.1021/acs.joc.0c02575
J. Org. Chem. 2021, 86, 2431−2436

Table 1. ^{1}H (500 MHz) and $^{13}C\{^{1}H\}$ (125 MHz) NMR Data of Compounds 1, 2, 3, and 4 in Dimethyl Sulfoxide (DMSO) (δ ppm)

	1		2		3		4	
no.	δ_C	δ_H (J in Hz)	δ_C	δ_H (J in Hz)	δ_C	δ_H (J in Hz)	δ_C	δ_H (J in Hz)
1	NH	10.97, s	NH	10.76, s	NH	10.55, s	NH	11.97, s
2	147.2, C		154.6, C		153.4, C		172.1, C	
3	44.1, C		51.9, C		51.7, C		50.1, C	
4	40.0, C		39.1, C		39.1, C		39.0, C	
5	26.5, CH_2	2.12, m	26.7, CH_2	2.40, t (11.3)	26.7, CH_2	2.40, t (13.1)	26.6, CH_2	2.38, t (13.4)
		1.96, m		1.94, m		1.95, m		1.99, m
6	30.5, CH_2	2.14, m	30.6, CH_2	2.54, m	30.7, CH_2	2.55, m	30.4, CH_2	2.53, m
		1.92, m		1.93, m		1.94, m		2.19, m
7	93.4, C		94.1, C		94.1, C		93.9, C	
8	O		O		O		O	
9	83.6, CH	3.83, s	78.8, CH	4.72, s	78.8, CH	4.73, d (1.8)	83.8, CH	3.89, d (1.3)
10	196.3, C		196.4, C		196.5, C		197.7, C	
11	129.4, CH	6.45, s	120.4, CH	6.12, s	120.4, CH	6.13, s	120.8, CH	6.08, s
12	158.9, C		159.6, C		159.7, C		158.4, C	
13	77.6, C		77.5, C		77.6, C		77.8, C	
14	34.9, CH_2	2.14, m	32.0, CH_2	2.12, d (13.4)	32.1, CH_2	2.13, d (13.3)	31.6, CH_2	2.19, m
		2.20, m		1.75, td (11.7, 3.5)		1.78, td (12.8, 3.8)		1.74, td (12.3, 3.9)
15	15.6, CH_2	2.09, m	21.4, CH_2	1.90, m	21.4, CH_2	1.92, m	16.6, CH_2	1.91, m
				1.66, d (11.4)		1.67, d (12.0)		1.79, m
16	40.2, CH	2.28, m	48.9, CH	2.71, m	48.9, CH	2.72, m	59.3, CH	3.27, t (11.9)
17	91.6, CH	5.30, m	27.5, CH_2	2.61, dd (13.2, 6.3)	27.7, CH_2	2.61, dd (13.0, 6.3)	195.4, C	
				2.31, dd (12.7, 11.2)		2.31, dd (12.5, 11.7)		
18	99.1, CH	6.24, d (1.6)	115.6, C		115.3, C		116.0, C	
19	126.3, C		123.8, C		125.1, C		120.5, C	
20	121.1, CH	7.43, d (8.3)	119.1, CH	7.27, d (8.3)	118.1, CH	7.26, d (8.0)	120.9, CH	7.58, d (8.4)
21	119.1, CH	6.93, dd (8.4, 1.9)	119.3, CH	6.91, dd (8.4, 1.9)	118.9, CH	6.89, t (7.1)	122.2, CH	7.16, dd (8.4, 1.8)
22	125.3, C		124.2, C		119.7, CH	6.93, t (7.2)	127.2, C	
23	110.8, CH	7.36, d (1.9)	111.8, CH	7.26, d (1.8)	112.3, CH	7.26, d (8.0)	113.0, CH	7.46, d (1.4)
24	137.0, C		140.7, C		140.5, C		142.0, C	
25	24.9, CH_3	1.38, s	16.7, CH_3	1.31, s	16.8, CH_3	1.31, s	26.4, CH_3	1.57, s
26	22.3, CH_3	0.88, s	23.9, CH_3	1.01, s	23.9, CH_3	1.04, s	23.7, CH_3	1.06, s
27	68.7, CH_2	3.59, d (12.5)	64.9, CH_2	4.09, dd (13.3, 2.2)	64.9, CH_2	4.09, dd (10.4, 2.6)	67.7, CH_2	3.61, d (12.5)
		3.54, dd (12.5, 1.9)		3.69, d (13.2)		3.70, d (13.3)		3.55, dd (12.4,1.8)
28	64.6, C		75.6, C		75.6, C		65.6, C	
29	21.6, CH_3	0.80, s	17.4, CH_3	1.22, s	17.4, CH_3	1.22, s	21.2, CH_3	0.86, s
30			176.1, C		176.1, C			
31			72.0, C		72.0, C			
32			27.9, CH_3	1.38, s	27.9, CH_3	1.38, s		
33			27.8, CH_3	1.38, s	27.8, CH_3	1.38, s		
13-OH				5.15, s		5.13, s		5.29, s
17-OH		6.64, d (3.8)						
28-OH		5.30, s						5.32, s
31-OH				5.25, s		5.25, s		

assigning the 3*S*, 4*R*, 7*R*, 9*R*, 13*S*, 16*S*, 28*R* configuration of **2**. The relative configuration of **3** was also deduced as 3*S**, 4*R**, 7*R**, 9*R**, 13*S**, 16*S**, 28*R** according to the NOESY correlations (Figure S1), chemical shifts, and the proposed biogenetic relationships between compounds **2** and **3**. The absolute configuration of **3** was finally determined as 3*S*, 4*R*, 7*R*, 9*R*, 13*S*, 16*S*, 28*R* based on the similar ECD curves between **2** and **3**. Similarly, the relative configuration of **4** was deduced as 3*S**, 4*R**, 7*R**, 9*R**, 13*S**, 16*R**, 28*R** based on the NOESY correlations (Figure S2) of H-26 (δ_H 1.06)/H-16 (δ_H 3.27), H-25 (δ_H 1.57)/OH-13 (δ_H 5.29), H-26/H-27 (δ_H 3.61, 3.55), and H-27/H-11 (δ_H 6.08) and biogenetic considerations. The absolute configuration of **4** was determined to be 3*S*, 4*R*, 7*R*, 9*R*, 13*S*, 16*R*, 28*R* by computational ECD calculations (Figure 4).

Based on the structural feature of compound **1**, a possible biosynthetic pathway for **1** is proposed (Figure 6). Ascandinine D (**4**) was assumed to be the biogenetic precursor of **1**. Ascandinine D underwent a reduction reaction and a subsequent retro-aldol type C-17−C-18 cleavage to produce the C-17 aldehyde intermediate **B**, which subsequently underwent a hemiacetal-forming cyclization with the intramolecular 13-OH group to give ascandinine A (**1**).

Compounds **1**−**4** were evaluated for cytotoxicity against a series of cancer cell lines (Table 2), with only ascandinine D (**4**) active against the HL-60 cells with an IC_{50} value of 7.8 μM. The antiviral activity of ascandinines B−D (**2**−**4**) was

https://dx.doi.org/10.1021/acs.joc.0c02575
J. Org. Chem. 2021, 86, 2431−2436

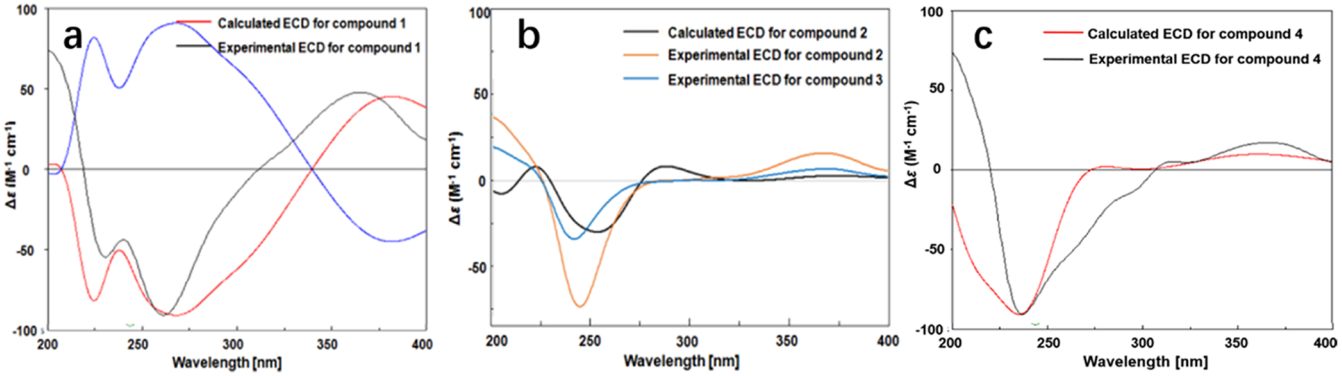

Figure 4. Experimental ECD spectra of **1**−**4** and the calculated ECD curves for (3*S*, 4*R*, 7*R*, 9*R*, 13*S*, 16*R*, 17*S*, 28*R*)-**1** (a), (3*S*, 4*R*, 7*R*, 9*R*, 13*S*, 16*S*, 28*R*)-**2** (b), and (3*S*, 4*R*, 7*R*, 9*R*, 13*S*, 16*R*, 28*R*)-**4** (c).

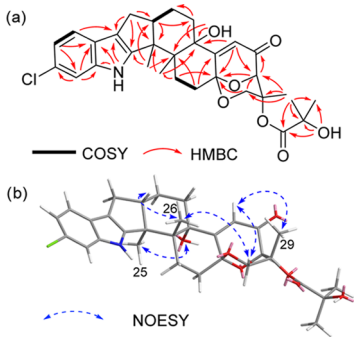

Figure 5. (a) COSY and key HMBC correlations and (b) key NOESY correlations for **2**.

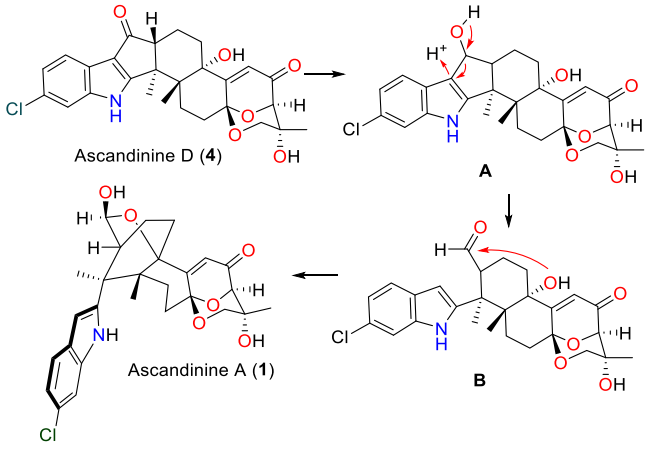

Figure 6. Proposed biogenetic pathway of compound **1**.

Table 2. Cytotoxicity of Compounds 1-4[a]

	IC_{50} (μM)				
compound	MGC-803	HCT-116	SH-SY5Y	Hela	HL-60
1	>30.0	>30.0	>30.0	>30.0	>30.0
2	>30.0	>30.0	>30.0	>30.0	>30.0
3	>30.0	>30.0	>30.0	>30.0	>30.0
4	>30.0	>30.0	>30.0	>30.0	7.8
ADR	0.2	0.2	0.1	0.6	0.02

[a]ADR = Adriamycin

evaluated against influenza A virus (H1N1) using the cytopathic effect (CPE) inhibition assay (Table 3, due to the lack of sample, compound **1** was not tested), and compound **3** exhibited inhibitory effects with an IC_{50} value of 26 μM (ribavirin as a positive control, IC_{50} = 31 μM).

Table 3. Antiviral Activities of Anti-Influenza A (H1N1) Virus for 2−4

	2	3	4	Ribavirin
IC_{50} (μM)	>150	26	>150	31

CONCLUSIONS

Paxilline-type indole terpenoids were first discovered in the mid of 1960s, sharing a highly conserved indole-containing 6/5/5/6/6/6 core skeleton, with over 100 analogues reported to date.[2,4−6,18] In this research, four new paxilline-like indole diterpenoids were isolated from an Antarctic sponge-derived fungus *A. candidus* HDN15-152. Ascandinine A (**1**) is the first case of a paxilline-type indole terpenoid derivative with C-17−C-18 carbon bond cleavage resulting in an unprecedented 2-oxabicyclo[2.2.2]octan-3-ol-containing skeleton, and with a hemiacetal moiety at C-16. Compounds **2**−**4** also represent a rare type of indole diterpene skeleton characterized by the 6/5/5/6/6/6/6-fused ring system with only four cases (asperindoles A−D) known.[4] Additionally, paxilline-type indole terpenoids with C-17 oxygenation as a carbonyl are rare, with only one natural product (penerpene H) reported.[5]

EXPERIMENTAL SECTION

General Experimental Procedures. Specific rotations were obtained on a JASCO P-1020 digital polarimeter. UV spectra were recorded on a HITACHI 5430. CD spectra were measured on a JASCO J-715 spectropolarimeter. NMR spectra were recorded on an Agilent 500 MHz DD2 spectrometer (Agilent, Beijing, China) using tetramethylsilane as an internal standard, and the chemical shifts were recorded in δ values. HRESIMS were obtained using a Thermo Scientific LTQ Orbitrap XL mass spectrometer. Semipreparative HPLC was performed using an ODS column [HPLC (YMC-Pack ODS-A, 10 × 250 mm, 5 μm, 3 mL/min)]. Medium-pressure preparation liquid chromatography (MPLC) was performed on a Bonna-Agela CHEETAH HP100 (Beijing Agela Technologies Co., Ltd.). Column chromatography (CC) was performed with silica gel (100−200 mesh, 200−300 mesh, Qingdao Marine Chemical Inc.) and Sephadex LH-20 (Amersham Biosciences), respectively.

Fungal Material. The fungal strain *A. candidus* HDN15-152 was isolated from the sponge collected from Pulitzer bay, Antarctica. It was identified by the ITS sequence and the sequence data have been submitted to GenBank (accession number: MH430037). The voucher specimen was deposited in our laboratory at −20 °C.

https://dx.doi.org/10.1021/acs.joc.0c02575
J. Org. Chem. 2021, 86, 2431−2436

Fermentation and Extraction. The fungus *A. candidus* HDN15-152 was cultured under static conditions at 28 °C in 1 L Erlenmeyer flasks containing 300 mL of the culture medium comprising 4% soluble starch, 0.2% monosodium glutamate, 3% maltose, 0.1% yeast extract, 3% saccharose, 0.05% soybean meal, 0.03% magnesium sulfate heptahydrate, 0.05% monopotassium phosphate, and 0.2% peptone (in seawater). After 30 days of cultivation, 30 L of whole broth was filtered through cheesecloth to separate the supernatant from the mycelia. The former was extracted three times with EtOAc, while the latter was extracted three times with methanol and concentrated under reduced pressure to afford an aqueous solution, which was extracted three times with EtOAc. Both EtOAc solutions were combined and concentrated under reduced pressure to give the organic extract (35.5 g).

Isolation. The crude extract was applied on a VLC column using a stepped gradient elution of MeOH-CH_2Cl_2, yielding eight subfractions (Fr.1-Fr.8). Fr.3 was applied on a C-18 ODS column using a step gradient elution of MeOH/H_2O yielding five subfractions (Fr.3.1-Fr.3.5). Fr.3.4 eluted with methyl alcohol was separated by MPLC (C-18 ODS) using a step gradient elution of MeOH-H_2O (50:50 to 100:0) to furnish eight subfractions (Fr.3.4.1-Fr.3.4.8). Fr.3.4.5 was purified by semipreparative HPLC (70:30 MeOH/H_2O, 3 mL/min) to afford compound **1** (1.5 mg, t_R 25.0 min). Fr.3.4.8 was subjected to semipreparative HPLC (80:20 MeOH/H_2O, 3 mL/min) to furnish two subfractions (Fr.3.4.8.1-Fr.3.4.8.2). Fr.3.4.8.1 was further purified by semipreparative HPLC (52:48 MeCN/H_2O, 3 mL/min) to afford compound **2** (8.0 mg, t_R 15.0 min). Fr.3.4.8.2 was subjected to semipreparative HPLC (80:20 MeOH/H_2O, 3 mL/min) to afford compound **3** (4.0 mg, t_R 15.0 min). Fr.4 eluted with methyl alcohol was separated by MPLC (C-18 ODS) using a step gradient elution of MeOH-H_2O (40:60 to 100:0) to furnish 10 subfractions (Fr.4.1-Fr.4.10). Fr.4.7 was further purified by semipreparative HPLC (60:40 MeOH/H_2O, 3 mL/min) to afford compound **4** (1.5 mg, t_R 32.0 min).

*Ascandinine A (**1**).* White solid; $[\alpha]_D^{20}$ +11 (*c* 1.00, MeOH); CD (MeOH) λ_{max} ($\Delta\varepsilon$) 229 (−12.4), 240 (−7.8), 261 (−18.8), 365 (+9.8); UV (MeOH) λ_{max} (log ε): 229 (3.82), 275 (1.78) nm; ^{1}H and ^{13}C NMR data, see Table 1; HRMS (ESI) *m/z*: $[M + H]^+$ calcd for $C_{27}H_{31}ClNO_6$ 500.1834; found 500.1835.

*Ascandinine B (**2**).* Yellow solid; $[\alpha]_D^{20}$ +33 (*c* 0.93, MeOH); CD (MeOH) λ_{max} ($\Delta\varepsilon$) 244 (−11.5), 369 (+2.45); UV (MeOH) λ_{max} (log ε): 237 (5.15), 284 (1.03) nm; ^{1}H and ^{13}C NMR data, see Table 1; HRMS (ESI) *m/z*: $[M + H]^+$ calcd for $C_{31}H_{37}ClNO_7$, 570.2253; found 570.2251.

*Ascandinine C (**3**).* Yellow solid; $[\alpha]_D^{20}$ +74 (*c* 0.33, MeOH); CD (MeOH) λ_{max} ($\Delta\varepsilon$) 241 (−9.3), 370 (+2.0); UV (MeOH) λ_{max} (log ε): 228 (5.34) nm; ^{1}H and ^{13}C NMR data, see Table 1; HRMS (ESI) *m/z*: $[M + H]^+$ calcd for $C_{31}H_{38}NO_7$, 536.2643; found 536.2641.

*Ascandinine D (**4**).* White solid; $[\alpha]_D^{20}$ +4 (*c* 1.00, MeOH); CD (MeOH) λ_{max} ($\Delta\varepsilon$) 237 (−6.3), 369 (+1.2); UV (MeOH) λ_{max} (log ε): 220 (5.89), 240 (3.43) nm; ^{1}H and ^{13}C NMR data, see Table 1; HRMS (ESI) *m/z*: $[M + H]^+$ calcd for $C_{27}H_{29}ClNO_6$, 498.1678; found 498.1673.

Computation Section. Conformational searches were run by employing the "systematic" procedure implemented in Spartan'14 using MMFF (Merck molecular force field).[19] All MMFF minima were reoptimized with DFT calculations at the B3LYP/6-31+G(d) level using the Gaussian09 program.[20] The geometry was optimized starting from various initial conformations, with vibrational frequency calculations confirming the presence of minima. Time-dependent DFT calculations were performed on two lowest-energy conformations for (3*S*, 4*R*, 7*R*, 9*R*, 13*S*, 16*R*, 17*S*, 28*R*)-**1**, five lowest-energy conformations for (3*S*, 4*R*, 7*R*, 9*R*, 13*S*, 16*S*, 28*R*)-**2**, and one lowest-energy conformation for (3*S*, 4*R*, 7*R*, 9*R*, 13*S*, 16*R*, 28*R*)-**4** (>5% population) using 30 excited states and using a polarizable continuum model (PCM) for MeOH. ECD spectra were generated using the program SpecDis[21] by applying a Gaussian band shape with 0.25 eV width for **1**, 0.30 eV width for **2**, and 0.35 eV for **4**, from dipole length rotational strengths. The dipole velocity forms yielded negligible differences. The spectra of the conformers were combined using Boltzmann weighting, with the lowest-energy conformations accounting for about 99% of the weights. The calculated spectra were shifted by 5 nm for **1**, 10 nm for **2**, and 10 nm for **4** to facilitate comparison to the experimental data.

Biological Assay. Cytotoxicity activities of **1**−**4** were evaluated against HL-60 and (using the MTT method) and Hela, HCT-116, SH-SY5Y, and MGC-803 (using the SRB method). The antiviral activities of compounds **2**−**4** against influenza A virus (H1N1) were evaluated by the CPE inhibition assay. The detailed methodologies for biological testing have been described in our previous report.[22,23]

■ ASSOCIATED CONTENT

Supporting Information

The Supporting Information is available free of charge at https://pubs.acs.org/doi/10.1021/acs.joc.0c02575.

COSY, HMBC, and NOESY correlations of **3** and **4**, HRESIMS and NMR spectra of **1**−**4**, IR spectra of **1**−**4**, and computational calculation details (PDF)

■ AUTHOR INFORMATION

Corresponding Authors

Tianjiao Zhu − *Key Laboratory of Marine Drugs, Chinese Ministry of Education, School of Medicine and Pharmacy, Ocean University of China, Qingdao 266003, P. R. China*; Email: zhutj@ouc.edu.cn

Dehai Li − *Key Laboratory of Marine Drugs, Chinese Ministry of Education, School of Medicine and Pharmacy, Ocean University of China, Qingdao 266003, P. R. China; Laboratory for Marine Drugs and Bioproducts and Open Studio for Druggability Research of Marine Natural Products, Pilot National Laboratory for Marine Science and Technology, Qingdao 266237, P. R. China*; orcid.org/0000-0002-7191-2002; Phone: 0086-532-82031619; Email: dehaili@ouc.edu.cn; Fax: 0086-532-82033054

Authors

Guoliang Zhou − *Key Laboratory of Marine Drugs, Chinese Ministry of Education, School of Medicine and Pharmacy, Ocean University of China, Qingdao 266003, P. R. China*

Chunxiao Sun − *Key Laboratory of Marine Drugs, Chinese Ministry of Education, School of Medicine and Pharmacy, Ocean University of China, Qingdao 266003, P. R. China*

Xuewen Hou − *Key Laboratory of Marine Drugs, Chinese Ministry of Education, School of Medicine and Pharmacy, Ocean University of China, Qingdao 266003, P. R. China*

Qian Che − *Key Laboratory of Marine Drugs, Chinese Ministry of Education, School of Medicine and Pharmacy, Ocean University of China, Qingdao 266003, P. R. China*; orcid.org/0000-0003-0610-1593

Guojian Zhang − *Key Laboratory of Marine Drugs, Chinese Ministry of Education, School of Medicine and Pharmacy, Ocean University of China, Qingdao 266003, P. R. China; Laboratory for Marine Drugs and Bioproducts, Pilot National Laboratory for Marine Science and Technology, Qingdao 266237, P. R. China*

Qianqun Gu − *Key Laboratory of Marine Drugs, Chinese Ministry of Education, School of Medicine and Pharmacy, Ocean University of China, Qingdao 266003, P. R. China*

Chenguang Liu − *College of Marine Life Sciences, Ocean University of China, Qingdao 266003, P. R. China*

Complete contact information is available at: https://pubs.acs.org/10.1021/acs.joc.0c02575

https://dx.doi.org/10.1021/acs.joc.0c02575
J. Org. Chem. 2021, 86, 2431−2436

Notes

The authors declare no competing financial interest.

■ ACKNOWLEDGMENTS

This work was financially supported by the National Key R&D Program of China (grant 2018YFC1406705), the National Natural Science Foundation of China (41876216, 81973234, and 81991522), the National Science and Technology Major Project for Significant New Drugs Development (2018ZX09735004), the Marine S&T Fund of Shandong Province for Pilot National Laboratory for Marine Science and Technology (Qingdao) (2018SDKJ0401-2), the Project funded by China Postdoctoral Science Foundation (2017M622286), and the Taishan Scholar Youth Expert Program in Shandong Province (tsqn201812021). The authors also thank Dr. R.A. Keyzers for help with preparation of the manuscript.

■ REFERENCES

(1) Saikia, S.; Nicholson, M. J.; Young, C.; Parker, E. J.; Scott, B. The Genetic Basis for Indole-diterpene Chemical Diversity in Filamentous Fungi. *Mycol. Res.* **2008**, *112*, 184−199.

(2) Reddy, P.; Guthridge, K.; Vassiliadis, S.; Hemsworth, J.; Hettiarachchige, I.; Spangenberg, G.; Rochfort, S. Tremorgenic Mycotoxins: Structure Diversity and Biological Activity. *Toxins* **2019**, *11*, No. 302.

(3) Moldes-Anaya, A.; Rundberget, T.; Uhlig, S.; Rise, F.; Wilkins, A. L. Isolation and Structure Elucidation of Secopenitrem D, an Indole Alkaloid from *Penicillium crustosum* Thom. *Toxicon* **2011**, *57*, 259−265.

(4) Ivanets, E. V.; Yurchenko, A. N.; Smetanina, O. F.; Rasin, A. B.; Zhuravleva, O. I.; Pivkin, M. V.; Popov, R. S.; Amsberg, G. V.; Afiyatullov, S. S.; Dyshlovoy, S. A. Asperindoles A-D and a *p*-Terphenyl Derivative from the Ascidian-Derived Fungus *Aspergillus* sp. KMM 4676. *Mar. Drugs* **2018**, *16*, No. 232.

(5) Zhou, L. M.; Kong, F. D.; Fan, P.; Ma, Q. Y.; Xie, Q. Y.; Li, J. H.; Zheng, H. Z.; Zheng, Z. H.; Yuan, J. Z.; Dai, H. F.; Luo, D. Q.; Zhao, Y. X. Indole-Diterpenoids with Protein Tyrosine Phosphatase Inhibitory Activities from the Marine-Derived Fungus *Penicillium* sp. KFD28. *J. Nat. Prod.* **2019**, *82*, 2638−2644.

(6) Kong, F. D.; Fan, P.; Zhou, L. M.; Ma, Q. Y.; Xie, Q. Y.; Zheng, H. Z.; Zheng, Z. H.; Zhang, R. S.; Yuan, J. Z.; Dai, H. F.; Luo, D. Q.; Zhao, Y. X. Penerpenes A−D, Four Indole Terpenoids with Potent Protein Tyrosine Phosphatase Inhibitory Activity from the Marine-Derived Fungus *Penicillium* sp. KFD28. *Org. Lett.* **2019**, *21*, 4864−4867.

(7) Gao, S. S.; Li, X. M.; Williams, K.; Proksch, P.; Ji, N. Y.; Wang, B. G. Rhizovarins A-F, Indole-Diterpenes from the Mangrove-Derived Endophytic Fungus *Mucor irregularis* QEN-189. *J. Nat. Prod.* **2016**, *79*, 2066−2074.

(8) Sun, K.; Li, Y.; Guo, L.; Wang, Y.; Liu, P.; Zhu, W. Indole Diterpenoids and Isocoumarin from the Fungus, *Aspergillus flavus*, Isolated from the Prawn, *Penaeus vannamei*. *Mar. Drugs* **2014**, *12*, 3970−3981.

(9) Munday-Finch, S. C.; Wilkins, A. L.; Miles, C. O.; Ede, R. M.; Thomson, R. A. Structure Elucidation of Lolitrem F, a Naturally Occurring Stereoisomer of the Tremorgenic Mycotoxin Lolitrem B, Isolated from *Lolium Perenne* Infected with *Acremonium Lolii*. *J. Agric. Food Chem.* **1996**, *44*, 2782−2788.

(10) Knaus, H. G.; McManus, O. B.; Lee, S. H.; Schmalhofer, W. A.; Garcia-Calvo, M.; Helms, L. M. H.; Sanchez, M.; Giangiacomo, K.; Reuben, J. P.; Smith, A. B.; Kaczorowski, G. J.; Garcia, M. L. Tremorgenic Indole Alkaloids Potently Inhibit Smooth Muscle High-Conductance Calcium-Activated Potassium Channels. *Biochemistry* **1994**, *33*, 5819−5828.

(11) Uhlig, S.; Botha, C. J.; Vrålstad, T.; Rolén, E.; Miles, C. O. Indole-Diterpenes and Ergot Alkaloids in *Cynodon dactylon* (Bermuda Grass) Infected with *Claviceps cynodontis* from an Outbreak of Tremors in Cattle. *J. Agric. Food Chem.* **2009**, *57*, 11112−11119.

(12) Smetanina, O. F.; Kalinovsky, A. I.; Khudyakova, Y. V.; Pivkin, M. V.; Dmitrenok, P. S.; Fedorov, S. N.; Ji, H.; Kwak, J. Y.; Kuznetsova, T. A. Indole Alkaloids Produced by a Marine Fungus Isolate of *Penicillium janthinellum* Biourge. *J. Nat. Prod.* **2007**, *70*, 906−909.

(13) Fan, Y.; Wang, Y.; Liu, P.; Fu, P.; Zhu, T.; Wang, W.; Zhu, W. Indole-Diterpenoids with Anti-H1N1 Activity from the Aciduric Fungus *Penicillium camemberti* OUCMDZ-1492. *J. Nat. Prod.* **2013**, *76*, 1328−1336.

(14) Zhou, H. B.; Li, L. Y.; Wang, W.; Che, Q.; Li, D. H.; Gu, Q. Q.; Zhu, T. J. Chrodrimanins I and J from the Antarctic Moss-Derived Fungus *Penicillium funiculosum* GWT2-24. *J. Nat. Prod.* **2015**, *78*, 1442−1445.

(15) Zhang, T.; Zhu, M. L.; Sun, G. Y.; Li, N.; Gu, Q. Q.; Li, D. H.; Che, Q.; Zhu, T. J. Exopisiod B and Farylhydrazone C, Two New Alkaloids from the Antarctic-Derived Fungus *Penicillium* sp. HDN14-431. *J. Asian Nat. Prod. Res.* **2016**, *18*, 959−965.

(16) Liu, C. C.; Zhang, Z. Z.; Feng, Y. Y.; Gu, Q. Q.; Li, D. H.; Zhu, T. J. Secondary Metabolites from Antarctic Marine-Derived Fungus *Penicillium crustosum* HDN153086. *Nat. Prod. Res.* **2019**, *33*, 414−419.

(17) Ma, X.; Peng, J.; Wu, G.; Zhu, T.; Li, G.; Gu, Q.; Li, D. Speradines B-D, Oxygenated Cyclopiazonic Acid Alkaloids from the Sponge-Derived Fungus *Aspergillus flavus* MXH-X104. *Tetrahedron* **2015**, *71*, 3522−3527.

(18) Zou, Y.; Smith, A. B. Total Synthesis of Architecturally Complex Indole Terpenoids: Strategic and Tactical Evolution. *J. Antibiot.* **2018**, *71*, 185−204.

(19) *Spartan 04*, Wavefunction Inc.: Irvine, CA, 2004.

(20) Frisch, M. J.; Trucks, G. W.; Schlegel, H. B.; Scuseria, G. E.; Robb, M. A.; Cheeseman, J. R.; Scalmani, G.; Barone, V.; Mennucci, B.; Petersson, G. A.; Nakatsuji, H.; Caricato, M.; Li, X.; Hratchian, H. P.; Izmaylov, A. F.; Bloino, J.; Zheng, G.; Sonnenberg, J. L.; Hada, M.; Ehara, M.; Toyota, K.; Fukuda, R.; Hasegawa, J.; Ishida, M.; Nakajima, T.; Honda, Y.; Kitao, O.; Nakai, H.; Vreven, T.; Montgomery, J. A.; Peralta, J. E.; Ogliaro, F.; Bearpark, M.; Heyd, J. J.; Brothers, E.; Kudin, K. N.; Staroverov, V. N.; Kobayashi, R.; Normand, J.; Raghavachari, K.; Rendell, A.; Burant, J. C.; Iyengar, S. S.; Tomasi, J.; Cossi, M.; Rega, N.; Millam, J. M.; Klene, M.; Knox, J. E.; Cross, J. B.; Bakken, V.; Adamo, C.; Jaramillo, J.; Gomperts, R.; Stratmann, R. E.; Yazyev, O.; Austin, A. J.; Cammi, R.; Pomelli, C.; Ochterski, J. W.; Martin, R. L.; Morokuma, K.; Zakrzewski, V. G.; Voth, G. A.; Salvador, P.; Dannenberg, J. J.; Dapprich, S.; Daniels, A. D.; Farkas, O.; Foresman, J. B.; Ortiz, J. V.; Cioslowski, J.; Fox, D. J. *Gaussian 09*, Revision B.01; Gaussian, Inc.: Wallingford CT, 2010.

(21) Bruhn, T.; Hemberger, Y.; Schaumlöffel, A.; Bringmann, G. *SpecDis*, Version 1.53, University of Wuerzburg: Germany, 2011.

(22) Du, L.; Zhu, T. J.; Liu, H. B.; Fang, Y. C.; Zhu, W. M.; Gu, Q. Q. Cytotoxic Polyketides from a Marine-Derived Fungus *Aspergillus glaucus*. *J. Nat. Prod.* **2008**, *71*, 1837−1842.

(23) Peng, J. X.; Jiao, J. Y.; Li, J.; Wang, W.; Gu, Q. Q.; Zhu, T. J.; Li, D. H. Pyronepolyene C-Glucosides with NF-κB Inhibitory and Anti-Influenza A Viral (H1N1) Activities from the Sponge-Associated Fungus *Epicoccum* sp. JJY40. *Bioorg. Med. Chem. Lett.* **2012**, *22*, 3188−3190.

https://dx.doi.org/10.1021/acs.joc.0c02575
J. Org. Chem. 2021, 86, 2431−2436